Differences in Multipath Propagation Between Urban and Suburban Environments:

Alexander Steingass, *German Aerospace Center (DLR)*
Andreas Lehner, *German Aerospace Center (DLR)*

BIOGRAPHY

Alexander Steingass was born in Mettmann, Germany in 1969. He received his Dipl Ing diploma in Electrical Engineering in 1997 (University of Ulm, Germany). Since then he has been a research scientist at the German Aerospace Center DLR - Institute of Communications and Navigation. He has been involved in several projects in the area of satellite navigation and location-dependent mobile services. In 2002, he was promoted to Dr. Ing. at the University of Essen.
Homepage: http://www.dlr.de/kn/kn-s/steingass
E-mail: alexander.steingass@dlr.de

Andreas Lehner was born in Gmunden, Austria in 1973. He received his diploma engineering degree in Mechatronics from the University of Linz, Austria in 2001. Since then he has been a research scientist at the German Aerospace Center DLR - Institute of Communications and Navigation. His research and project work focuses on multipath propagation and interference in satellite navigation systems. In 2007 he obtained the Dr. Ing. degree in Electrical Engineering from the University of Erlangen-Nuremberg, Germany.
Homepage http://www.dlr.de/kn/kn-s/lehner
E-mail: andreas.lehner@dlr.de.

ABSTRACT

In 2002 the German Aerospace Centre (DLR) performed a measurement campaign of the land mobile multipath channel. From this data a channel model was derived that is synthesising the measured channel impulse response. It allows the realistic simulation of the multipath channel by approximating every single reflection. This model includes time variant reflectors approaching and receding in dependency of the azimuth and elevation of the satellite. All the signal processing had been realised independently of the transmitted signal. Therefore the usability for both, navigation systems (GPS as well as GALILEO) and wideband communication systems is given.

1. INTRODUCTION

Besides the ionosphere one of the most significant problems to achieve an accurate navigation solution in urban and suburban environments with GPS or GALILEO is the multipath reception. Various channel models do exist for ground to ground communications (e.g. COST 207 for the GSM system). But there is still a lack of knowledge for broadband satellite to earth channels [1]. Therefore the German Aerospace Centre (DLR) performed a measurement campaign in 2002. In this campaign we used a Zeppelin to simulate a satellite transmitting a 100 MHz broadband signal towards earth. To ensure a realistic scenario the signal was transmitted between 1460 and 1560 MHz just nearby the GPS L1 band. This signal was received by a measurement van and was recorded using a regular time grid. The so gathered data was then passed through a super resolution algorithm to detect the single reflections. In a further step we tracked the detected reflections in time and gained a knowledge about the characteristics of any isolated reflection. This includes both Doppler shift and delay of the reflection. On top of this we gained knowledge about the direct path behaviour.

In this paper we will first describe the channel model itself to introduce the relevant parameters. In a separate section we will discuss the differences between the urban and the suburban case.

2. DIRECT PATH

In an open environment the direct path is represented by the line of sight (LOS) transmission of the signal. In a suburban environment this LOS signal is often blocked so that the first received path is attenuated and possibly delayed with respect to the LOS. In suburban environments we had been able to identify three major types of obstacles that influence the signal reception.

1. House fronts
2. Trees
3. Lampposts

2.1 The influence of house fronts

When the LOS ray is going to be blocked by a house front the signal is obviously affected. **Figure 1** shows the vehicle on a track during the measurement driving into the shadow of a building. The x-axis indicates the driven distance from start. At about 3886 m the vehicle is entering the shadowed area. From this instance on the signal is strongly attenuated. This behaviour is well known from the so called "Knife Edge Model" [2]. In this model it is assumed that a planar wave is hitting a half sided infinitively large plate. The calculated attenuation

from this model is also displayed in **Figure 1**. From this comparison the similarity of measurement and model is obvious. Therefore the knife edge model is selected to model this effect. This process is motion dependent only.
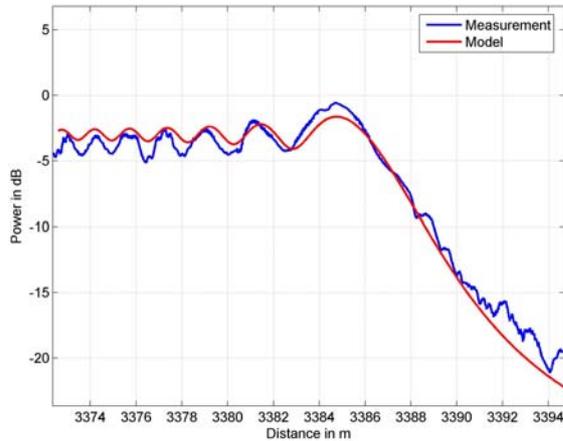
Figure 1: Diffraction by a house front measurement in comparison to the model used

2.2 The influence of trees

As it is shown in **Figure 2** the LOS signal can be attenuated by trees. The measured process on the one hand side is dependent on the length of the LOS path being within the tree top, on the other hand side an additional process is visible caused by branches and leafs. In contrast to approaches where branches and leafs are modelled as very complex scatterers [3] we use a combination of an attenuating only cylinder modelling the transmission through the tree and a statistical fading process modelling the branches and leafs. This process is motion dependent only.
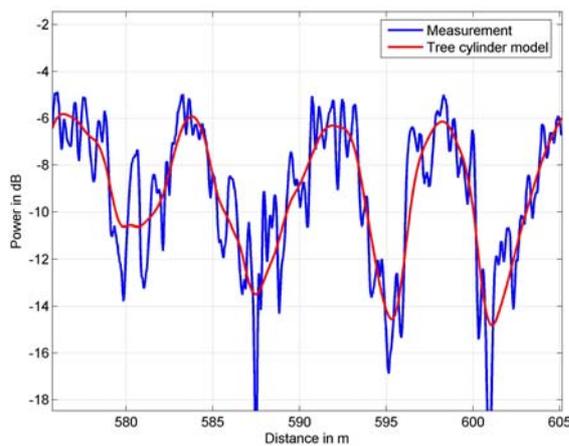
Figure 2: Signal attenuation by series of trees - comparison of measurement and cylinder model

2.3 The influence of lampposts

Surprisingly a lamppost has a strong effect on the LOS signal. Figure 3 shows an example of a lamppost with a diameter D of 20 cm. When passing by such a post the strength of the signal begins to oscillate, goes down quickly in the direct shadow of the post and comes up again oscillating behind.
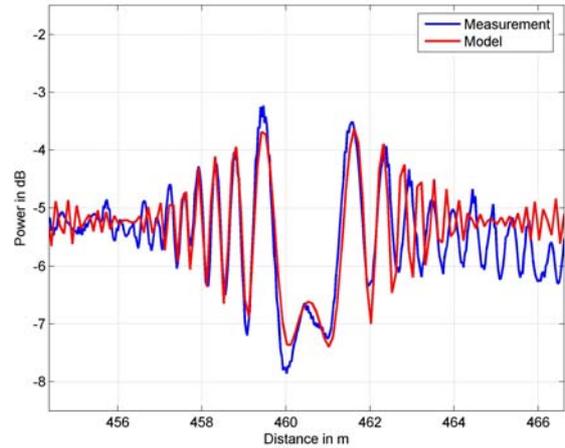
**Figure 3:** LOS signal being affected by a lamppost comparison of measurement and model

We model a lamppost with a "double knife edge model" where we assume two overlapping knife edge plates being present. One is reaching from −D/2<x<∞ and the other is reaching from −∞<x<D/2. Both edges are simulated separately and then added coherently. **Figure 3** shows the near perfect match of model and measurement. This process is also motion dependent only.

3. REFLECTED SIGNAL

In the measurement data many reflections appear in urban and suburban environment [4,5]. In contrast to ray tracing algorithms [6] we do not model a specific scenery. We assume reflections to be statistically distributed in the (x,y,z)-space and generate them statistically. In order to match the measured statistic we must take a closer look at the echo distribution.

3.1 Influence of the relative angle

Let us assume a receiver to be at position RX, a satellite at position S and a reflector at position R. Then the relative azimuth receiving angle α is the angle at the receiver illustrated in **Figure 4**.
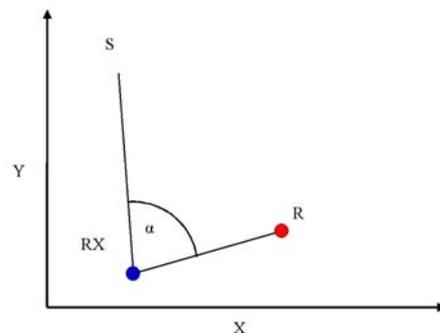
Figure 4: Definition of the angle α.
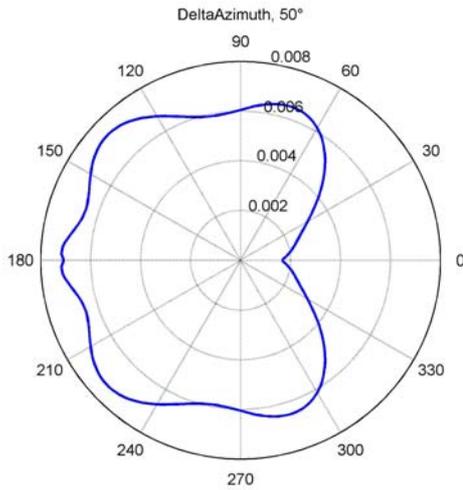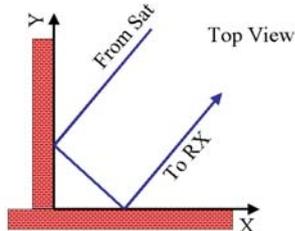
Figure 5: Likelihood distribution of the relative azimuth angle α in the suburban environment at 50° elevation.

We can see a clear dependency on the relative azimuth angle in the suburban measurement data (**Figure 5**) with a high likelihood for $60° < \alpha < 300°$. For this figure we averaged over all occurring absolute azimuth angles θ by

$$\overline{p}(\alpha) = \frac{\displaystyle\sum_{\theta_i} \frac{p(\alpha|\theta_i)}{p(\theta_i)}}{\displaystyle\sum_{\alpha_i}\sum_{\theta_i} \frac{p(\alpha_i|\theta_i)}{p(\theta_i)}} \qquad (1)$$

In contrast to the statistics for the urban environment published in [7], where a clear maximum exists for $\alpha = 180°$, the incidence angle of reflected signals is therefore varying much more in the suburban environment. In urban cities the rectangular structure of construction dominates. Due to this structure a corner reflector (see **Figure 6**) occurs very often. The main characteristic of this reflector is that a ray coming from a satellite is being reflected back into the satellite direction in the x-y plane. Its elevation is unchanged. Thus α is most likely to be around 180°. The suburban environment on the other hand side is more open, different kinds of construction and vegetation lead to a larger variety in position and back scatter angles of reflectors. Therefore the distribution of α is less pronounced.
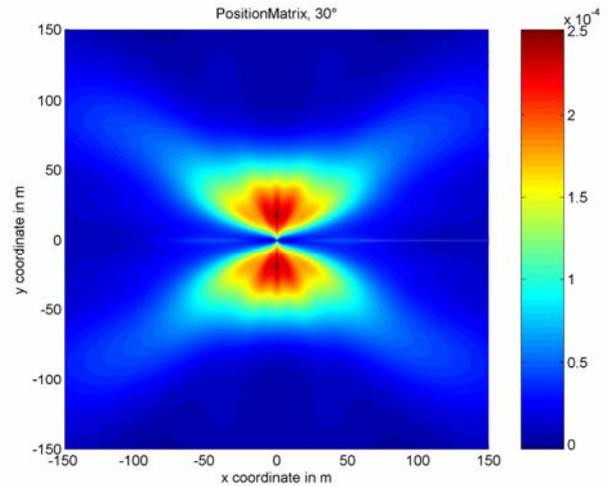

Figure 6: Corner reflector as it can be often found in urban environments.

3.2 Geometric occurrence of reflectors

Figure 7 shows the likelihood distribution of reflectors in a top view. In this figure the receiver is moving in x-

direction only. It can clearly be seen that the highest likelihood of receiving a reflector is when the reflector is on the right or on

Figure 7: Likelihood of reflectors being at a certain 2-D position for 30° elevation in the suburban environment. Moving direction of the receiver is in x-direction only.

the left side. The likelihood of receiving a reflector from the front is close to zero. This as well on the first look astonishing result becomes more plausible when one has a suburban street in mind. It must be unlikely that a reflecting obstacle is in near front position of the car, otherwise one would overrun it in the next second. To calculate the common likelihood of a reflector being present at a certain position for a specific satellite azimuth one has to multiply the statistically independent distributions shown in **Figure 5** and **Figure 7**. The result of this operation is shown in **Figure 8**, here the satellite position had been chosen at 25° azimuth. Comparing these results with the urban case published in [7], the 2D position distribution in **Figure 8** affirms the statements in the previous section, that the reflectors are much more distributed in the suburban environment.
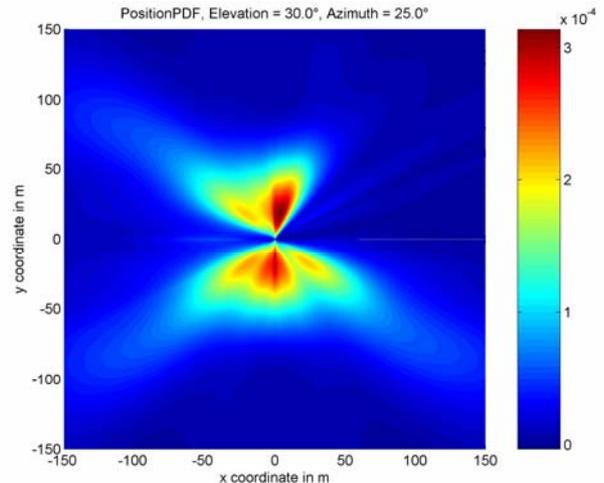
Figure 8: Common likelihood of reflectors being at a certain 2-D position. Satellite at 25° azimuth and 30° elevation.

3.3 Lifespan of reflectors

In the measurement data the channel appears rapidly changing. Many echoes disappear and others appear at new positions. This process is highly correlated to the receiver speed. When the car stops the reflections remain in the
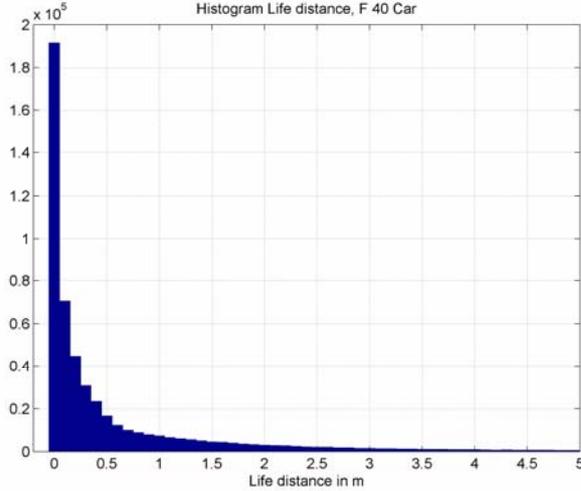

Figure 9: Life distance distribution of echoes

scenery. Therefore we defined a life distance of each reflector. This life distance is the distance the receiver is travelling until the echo disappears. **Figure 9** shows a histogram of the echo life distances. It can be seen that the life distance of the reflectors is usually well below 1 m. Most reflectors exist along a motion path below 5 m. Therefore the channel is changing rapidly.

3.4 Mean power of reflectors

Figure 10 shows the power distribution in dependency of the relative position. Since reflectors in the real world have a given geometrical size of course their distance plays a major role for the mean received power.
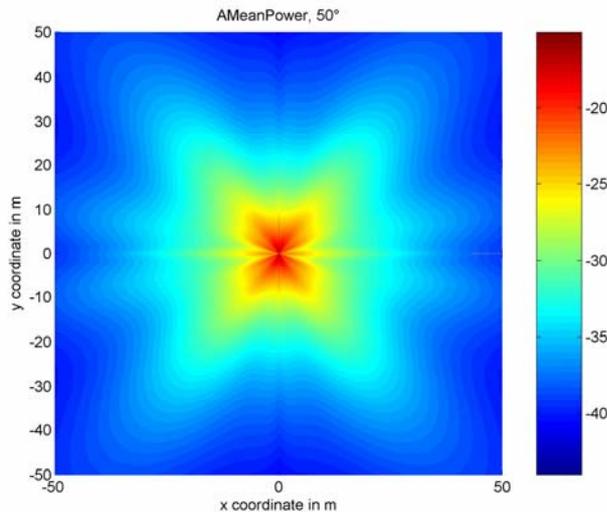
Figure 10: Mean power of the reflectors in dependency of their relative position.

Having again in mind the suburban street, it is quite understandable that the most powerful reflections are on the sides of the streets. With increasing distance the mean power of the reflections is decreasing. Beside the mean power map we have derived a power variance map (not shown) to allow a certain variation in this process, like we observed it in the measurements.

In comparison to the urban environment in [7], it is interesting to note that the mean power of echoes is 3-5 dB higher in the suburban case.

3.5 Fading process of reflections

When a car drives through a suburban environment, the receiver moves through a quasi stationary field radiated by the reflectors. Therefore the receiver recognises a variation of the actual power of the reflector (see also **Figure 12**). Interesting enough this fading process does not even come to a stop when the car does not move. We assume that the channel is changing for example due to trees in the wind and other cars. Furthermore there was no correlation between this fading process and the receiver speed. Therefore we assume this process to be time dependent only. The typical bandwidth of such a process is in the range of some Hertz. The deepness of the fades is expressed by the Rice factor K_{Rice}.

$$K_{Rice} = \frac{P_{const}}{P_{fad}} \qquad (2)$$

It defines the ratio between the constant power P_{const} and the power of the fading process P_{fad}. **Figure 11** shows the distribution of the Rice factor.
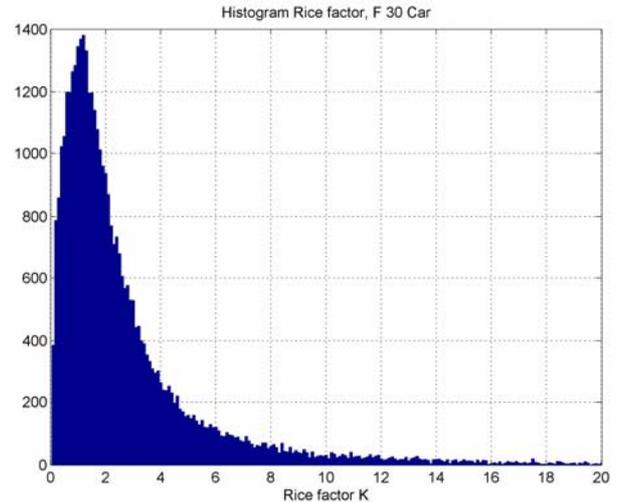

Figure 11: Rice factor histogram of the fading process.

3.6 Time series characteristic of reflectors

Classical channel models like the GSM channel model [8] use time invariant path delays and model the change of the reflector over the time by the assumption that many echoes are received at almost the same path delay and their absolute azimuth is equally distributed. The resulting Doppler spectrum, the so called Jakes spectrum [9], is given by:

$$S(f_D) = \begin{cases} \dfrac{const}{\sqrt{1 - \left(\dfrac{f_D}{f_{D\max}}\right)^2}} & \forall \ |f_D| < f_{D\max} \\[4ex] 0 & else \end{cases} \qquad (3)$$

This approach is feasible for narrow band systems like GSM but in a wide band system such as GPS/GALILEO we regard the modelling accuracy as insufficient. **Figure 12** shows the sliding window Fourier transform of an isolated reflection. There it can be seen that the echo is best characterised by a trace in Doppler frequency. Within 1.6 s the Doppler frequency of the echo changes from +30 Hz to -5 Hz. In the same period the path delay of the echo changes. The variability of the echo signal is clearly dependent on the vehicle speed. Therefore we implemented the channel model using a geometrical reflector representation. This means we initialise a reflector at a randomly chosen position (according to the measured statistics) and pass by with a receiver with the actual speed. Then both, path delay and phase of the echo can be calculated geometrically. This causes the main process to be motion dependent only. **Figure 13** shows how a single reflector is modelled. In terms of the reflector the artificial
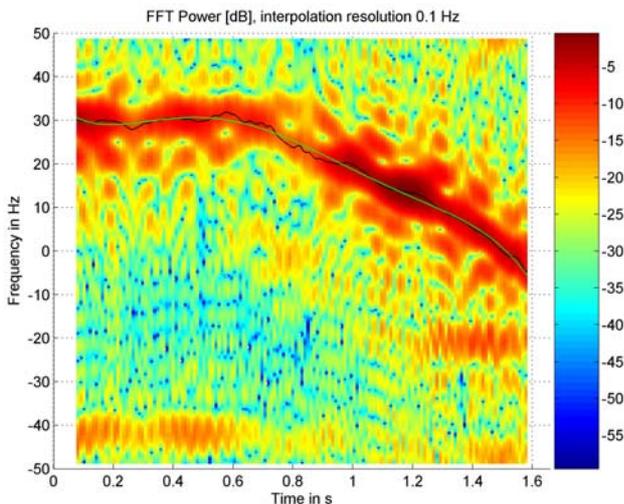
Figure 12: Sliding window Fourier transform of an isolated reflection.
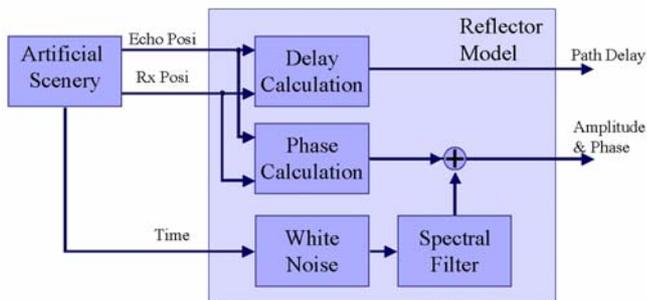

Figure 13: Model of an isolated reflector

scenery generates a continues series of receiver positions according to the actual speed. The receiver is moving only in x-direction. To simulate turns the relative azimuth of the satellite is changed.

3.7 Number of echoes

During a drive through a suburban environment the number of echoes being received changes. For a navigation receiver
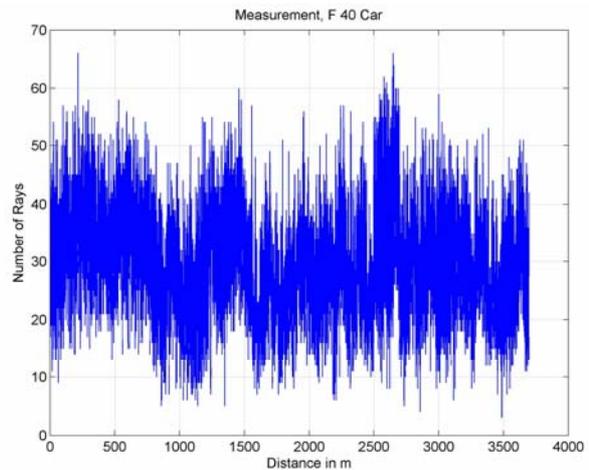

Figure 14: Number of coexisting echoes during a 15 minute drive trough a suburban environment.

that tries to estimate the channel impulse response (super resolution for multipath mitigation) a high number of reflections is a "high stress scenario". Other phases with a lower number of echoes are less critical. Besides the mean number of echoes it is therefore very important to exactly model this increasing and decreasing process. A sample of it is shown in **Figure 14**. Please note the relatively high number of echoes (up to 65) at the same time, which is even more than in the urban environment with up to 50 coexisting echoes (see [7]). We had been able to detect two processes: An extremely narrow band process with high power and a lower powered wide band process. Their combination results in a very good approximation of the process.

4. MODEL

The block diagram in **Figure 15** gives an overview of the implemented model. The x-coordinate and the relative satellite azimuth are derived from the user speed, user heading and satellite azimuth as explained in section 3.6.
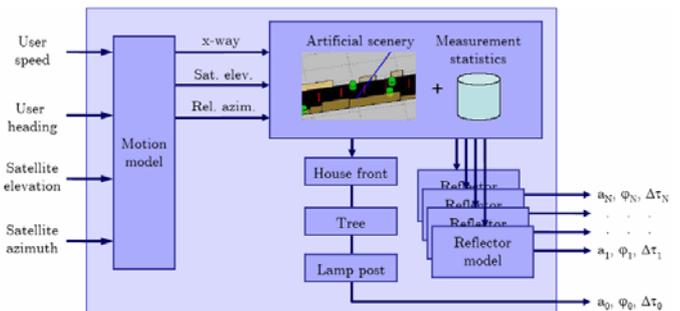

Figure 15: Block diagram of the channel model.

This drives the artificial scenery (**Figure 16**) where house fronts, trees and lampposts affect the direct path. Controlled by a number of echo generator the actual amount of reflections is created in the scenery at positions according to the likelihood distribution. These reflector positions are represented by the bubbles in **Figure 16**, where the echoes power is coded by
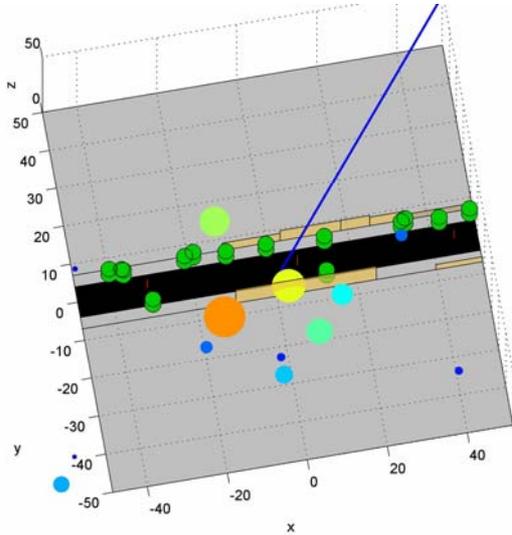

Figure 16: A picture of the artificial scenery with house fronts in brown, green cylindrical trees and red poles.

size and colour. The reflectors power, bandwidth, rice factor and lifespan are taken from the statistics. Their delay and phase is therefore changing according to this statistical parameters and according to the receiver movement relative to the reflector position. In **Figure 17** - **Figure 20** an example output of the channel model is given. In this scenario the car
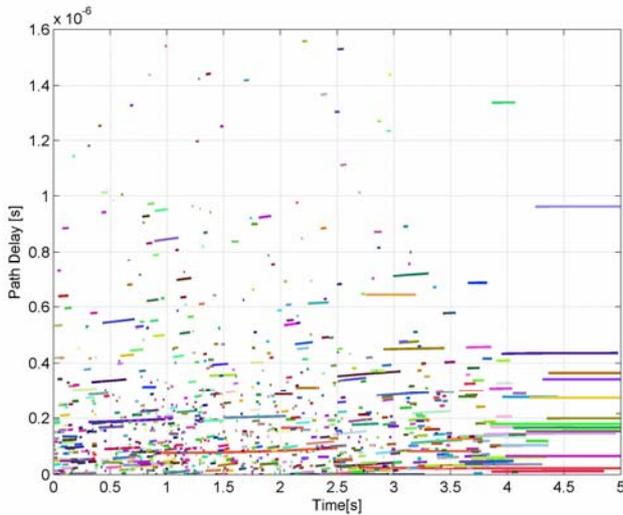
Figure 17: Example of generated echoes. Plotted is the path delay of the reflections over time.
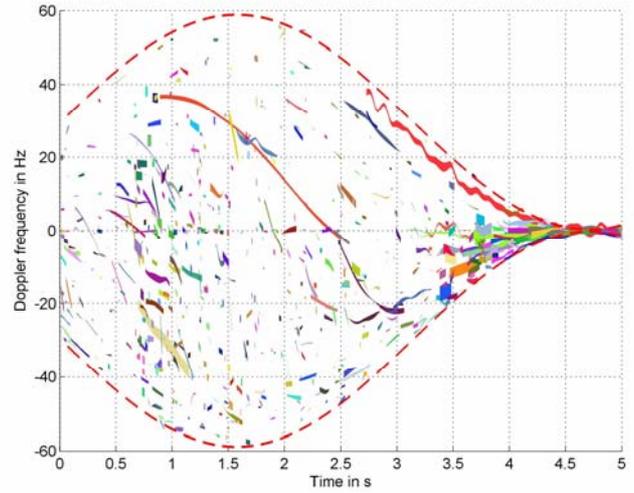
Figure 18: Example of generated echoes. Plotted is the Doppler of the reflections over time.

drives with a variable speed (using a sin(t) like stop and go function) through a suburban environment. At 4.7 s the speed of the vehicle is nearly 0 km/h. In **Figure 18** the Doppler shift of every echo is shown. The red dotted line is the theoretical limit for the Doppler shift given by

$$f_{Doppler} = \frac{\vec{v} \cdot \left(\overrightarrow{RX} - \vec{S} \right)}{c_0} f_C \qquad (4)$$

where v is the speed vector of the vehicle, RX is the receiver position, f_C is the carrier frequency, S is the satellite Position and c_0 is the speed of light. In this figure and in the detail (**Figure 20**) one can determine isolated echoes changing their Doppler shift during their life distance (for example the red coloured echo lasting from 0.9 - 2.5 s changing the Doppler from 35 to –5 Hz). The rapid changes in the channel are visible within the displayed period of around two seconds, where many echoes die and others are generated. Around the standstill the channel does not change much - clearly visible by the low Doppler bandwidth and the long lasting echoes (long lines) in **Figure 17**. In this situation only the time driven fading process is changing the channel. But neither an echo is terminated nor a new one is generated in this situation. Furthermore one can see regions where more echoes are present than in others.

Due to this precise modelling of reflections new receiver algorithms for e.g. multipath mitigation can be tested in very realistic simulations now. An important improvement compared to regular statistical models is the geometrical reflector representation which guarantees the realistic delay and phase correlation among the occurring echoes.
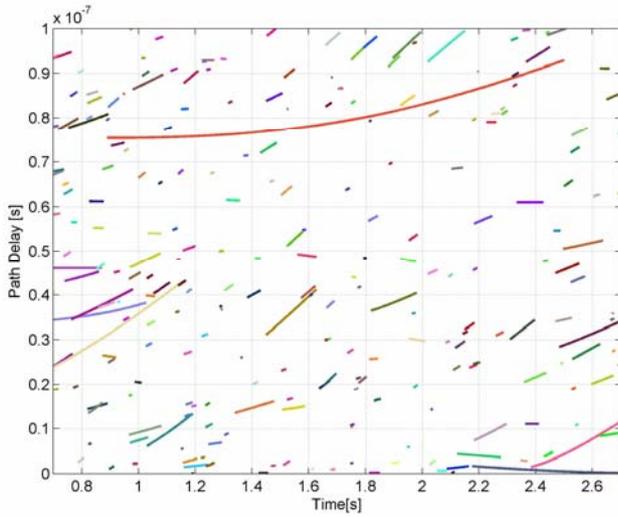
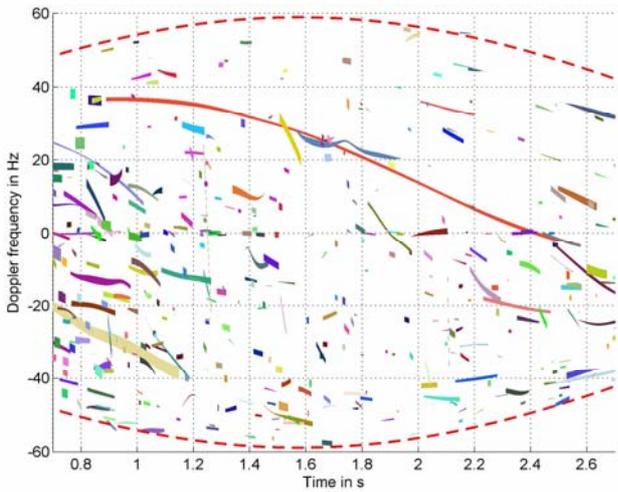**Figure 19:** Detail of **Figure 17**.

Figure 20: Detail of **Figure 18**.

5. COMPARISON BETWEEN URBAN AND SUBURBAN PROPAGATION

The direct comparison between the urban and suburban propagation case is done for the most relevant parameters:

- Mean Power of the reflections
- Geometrical distribution
- Relative angle distribution
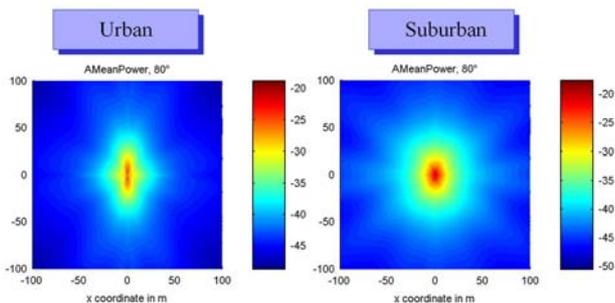- Number of coexisting Echoes

Figure 21: Mean power of reflections in dependency of their position – Comparison urban and suburban.
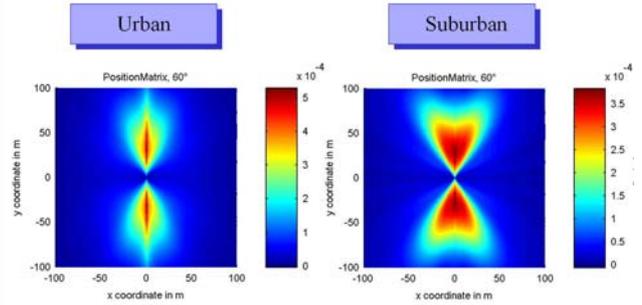

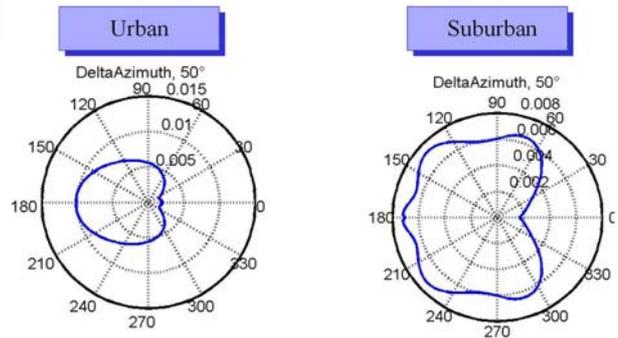**Figure 22:** Likelihood of occurrence in dependency of their position – Comparison urban and suburban.

Figure 23: Distribution of the relative angle (see **Figure 4**). – Comparison urban and suburban.
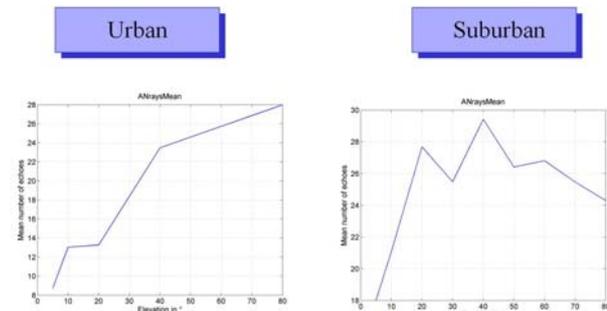

Figure 24: Number of coexisting Echoes – Comparison urban and suburban.

Figure 21 shows the mean power of reflections in dependency of their position. It can be seen that in the suburban case the echoes are stronger than in the urban case.

By comparing **Figure 25** and **Figure 28** this seems to be true for all elevations.

Figure 22 shows the likelihood distribution of the echoes in the x-y plane. It can clearly be seen that in the suburban case the echoes are wider distributed than in the urban case. We believe that this is a result of the more random city structure in suburban areas in contrast to the very regular and rectangular structures in the urban area.

The comparison of **Figure 26** and **Figure 29** is supporting this finding especially for mid elevations.

Figure 23 shows the distribution of the relative angle of arrival. It can clearly be seen that in the suburban case a much wider distribution occurs. Again we refer to the more random structure of suburban cities in the suburban case.

Again the elevation dependent comparison of **Figure 27** and **Figure 30** supports this trend especially in mid elevations.

Figure 24 shows the number of coexisting echoes in both cases in dependency of the elevation. This comparison shows clearly that in the suburban case there are much more reflections at the same time than in the urban case.

5. SUMMARY

In this paper we have presented our new channel model for the land mobile multipath channel. This channel model is based on a new approach: The combination of statistical data from a measurement and a deterministic scenario. The deterministic scenario is used for the direct path modelling. This includes effects such as shadowing by house fronts, tree attenuation and diffracting lampposts. The reflections of this channel model are generated statistically in the geometric scenario. Their generation is driven by data obtained from the measurement only. The model includes:

- Elevation changes,
- azimuth changes,
- speed changes
- and a variable number of reflectors.

The direct comparison between suburban and urban propagation shows four major differences:

- Echoes are stronger in suburban areas
- Echoes are wider distributed in suburban areas
- Relative angle is wider distributed in Suburban areas
- There are more coexisting echoes in suburban areas

The model is available for download:
http://www.kn-s.dlr.de/satnav/

REFERENCES

[1] Schweikert R., Wörz T.: "Signal design and transmission performance study for GNSS-2", Tech. note on digital channel model for data transmission, ESA, 1998.

[2] Orfanidis J. S.: "Electromagnetic Waves and Antennas", Internet www.ece.rutgers.edu/ orfanidi/ewa, Rutgers University, June 2004.

[3] Yvo L. C. de Jong and Matti H. A. J. Herben: "A tree-scattering model for improved propagation prediction in urban microcells", IEEE Transactions on Vehicular Technology, pages 503–513, March 2004.

[4] Steingass A., Lehner A.: "Measuring the navigation multipath channel a statistical analysis", ION GPS 2004 Conference Long Beach, California USA, September 2004.

[5] Steingass A., Lehner A.: "Measuring Galileo's multipath channel", Global Navigation Satellite Systems Conference (GNSS2003), Graz, Austria, 2003.

[6] Esbri-Rodriguez O., Konovaltsev A. and Hornbostel A.: "Modeling of the GNSS directional radio channel in urban areas based on synthetic environments", Proceedings of ION NTM, Jan. 2004.

[7] Lehner, A., Steingaß, A.: "A novel channel model for land mobile satellite navigation". Institute of Navigation Conference ION GNSS 2005, Long Beach, USA, September 13-16, 2005.

[8] COST 207 WG1: "Proposal on channel transfer functions to be used in GSM tests 1986", Technical report, CEPT Paris, 1986.

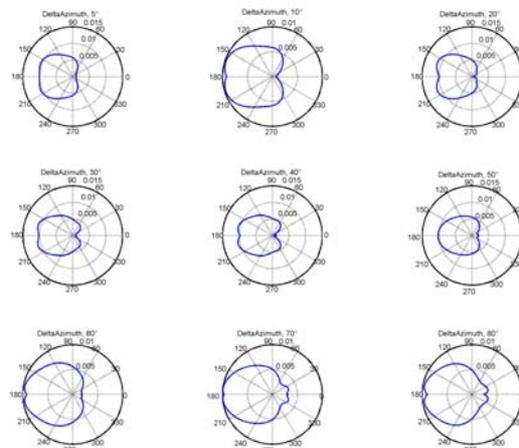[9] Jakes W. C.: "Microwave Mobile Communications", John Wiley & Sons, Inc. , New York, 1974.

Elevation dependent Analysis – Urban Case
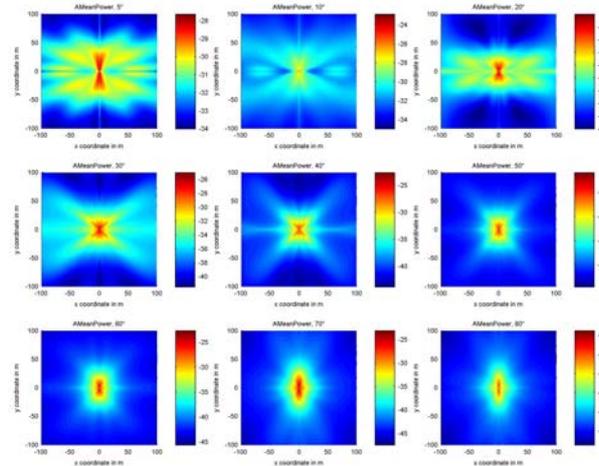
Figure 25: Mean power of reflections in dependency of their position – Urban case in dependency of the elevation
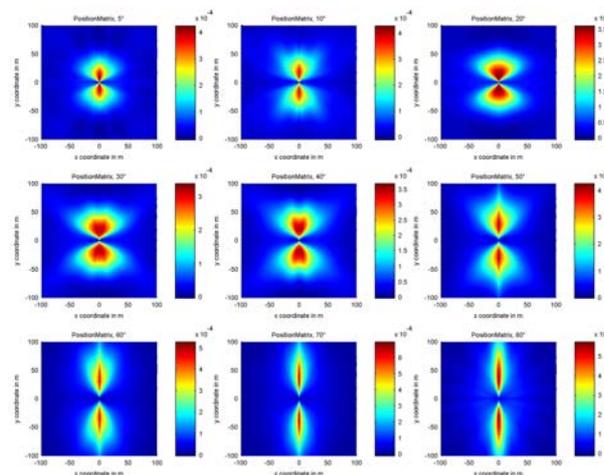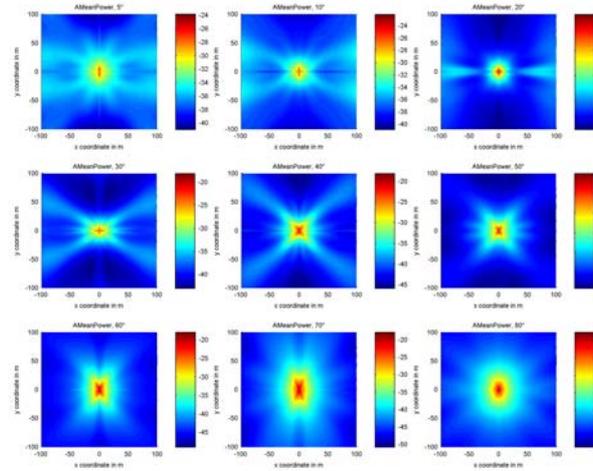

Figure 26: Likelihood of occurrence in dependency of their position – Urban case in dependency of the elevation
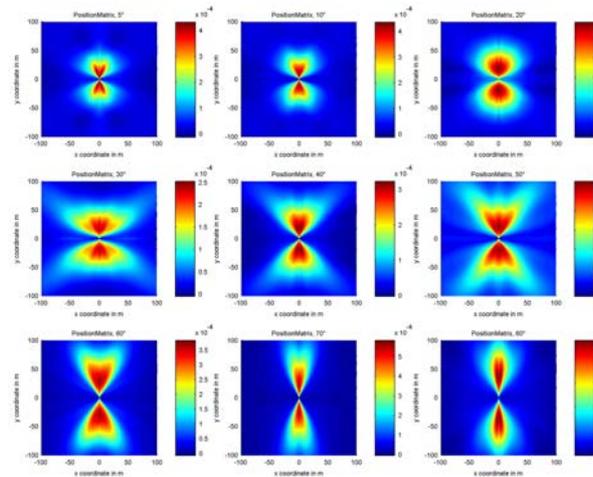

Figure 27: Distribution of the relative angle – Urban case in dependency of the elevation
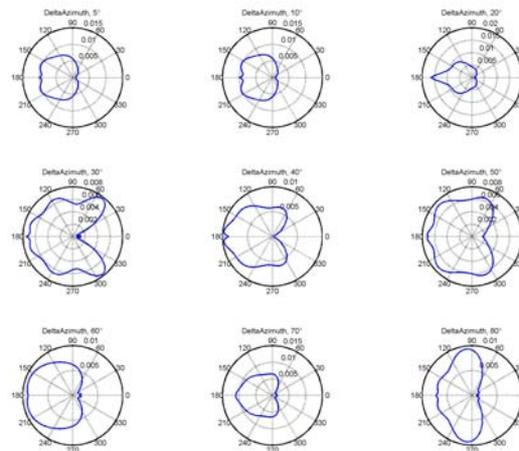
Elevation dependent Analysis – Suburban Case

Figure 28: Mean power of reflections in dependency of their position – Suburban case in dependency of the elevation

Figure 29: Likelihood of occurrence in dependency of their position – Suburban case in dependency of the elevation

Figure 30: Distribution of the relative angle – Suburban case in dependency of the elevation